

MIT Open Access Articles

*Optically Heralded Entanglement of
Superconducting Systems in Quantum Networks*

The MIT Faculty has made this article openly available. **Please share** how this access benefits you. Your story matters.

Citation: Krastanov, Stefan, Raniwala, Hamza, Holzgrafe, Jeffrey, Jacobs, Kurt, Lončar, Marko et al. 2021. "Optically Heralded Entanglement of Superconducting Systems in Quantum Networks." Physical Review Letters, 127 (4).

As Published: 10.1103/PHYSREVLETT.127.040503

Publisher: American Physical Society (APS)

Persistent URL: <https://hdl.handle.net/1721.1/143537>

Version: Final published version: final published article, as it appeared in a journal, conference proceedings, or other formally published context

Terms of Use: Article is made available in accordance with the publisher's policy and may be subject to US copyright law. Please refer to the publisher's site for terms of use.



Optically Heralded Entanglement of Superconducting Systems in Quantum Networks

Stefan Krastanov^{1,2}, Hamza Raniwala¹, Jeffrey Holzgrafe², Kurt Jacobs^{3,4}, Marko Lončar²,
Matthew J. Reagor⁵, and Dirk R. Englund^{1,6}

¹*Department of Electrical Engineering and Computer Science, Massachusetts Institute of Technology, Cambridge, Massachusetts 02139, USA*

²*John A. Paulson School of Engineering and Applied Sciences, Harvard University, Cambridge, Massachusetts 02138, USA*

³*U.S. Army Research Laboratory, Computational and Information Sciences Directorate, Adelphi, Maryland 20783, USA*

⁴*Department of Physics, University of Massachusetts at Boston, Boston, Massachusetts 02125, USA*

⁵*Rigetti Computing, 775 Heinz Avenue, Berkeley, California 94710, USA*

⁶*Research Laboratory of Electronics, Massachusetts Institute of Technology, Cambridge, Massachusetts 02139, USA*



(Received 27 January 2021; accepted 21 June 2021; published 22 July 2021)

Networking superconducting quantum computers is a longstanding challenge in quantum science. The typical approach has been to cascade transducers: converting to optical frequencies at the transmitter and to microwave frequencies at the receiver. However, the small microwave-optical coupling and added noise have proven formidable obstacles. Instead, we propose optical networking via heralding end-to-end entanglement with one detected photon and teleportation. This new protocol can be implemented on standard transduction hardware while providing significant performance improvements over transduction. In contrast to cascaded direct transduction, our scheme absorbs the low optical-microwave coupling efficiency into the heralding step, thus breaking the rate-fidelity trade-off. Moreover, this technique unifies and simplifies entanglement generation between superconducting devices and other physical modalities in quantum networks.

DOI: [10.1103/PhysRevLett.127.040503](https://doi.org/10.1103/PhysRevLett.127.040503)

A central challenge in quantum information science is to transfer quantum states between superconducting systems over long distances. The most widely investigated approach is microwave-optical (M-O) quantum state transduction [1–23]. However, despite concerted efforts in direct M-O transduction, it remains challenging to achieve a high transduction efficiency without adding significant noise [24]. Moreover, these problems are compounded because a full state transfer between two quantum devices requires sequential M-O and O-M transduction steps [25]. Here, we propose to replace these M-O-M steps with one round of optically heralded M-M entanglement, followed by state teleportation. In contrast to direct transduction, this photon-heralded entanglement scheme favors low M-O coupling efficiency to eliminate added noise, while assuring on-demand state teleportation by heralding and distilling M-M Bell pairs faster than their decoherence rates. Specifically, for present-day technology, we estimate entanglement rates exceeding 100 kHz per channel, an entanglement fidelity exceeding 0.99, and the potential for entanglement purification to reach a fidelity of 0.999 on present-day hardware. Our approach unifies and simplifies entanglement generation between superconducting devices and other physical modalities in quantum networks, including trapped ions, cold atoms, solid-state spin systems, or another traveling photon (corresponding to heralded M-O quantum state transduction). Crucially, our protocol does

not require the creation of new hardware: we show that today's transduction hardware can run our heralding scheme while providing orders of magnitude improvement in the networking fidelity compared to the typical deterministic transduction.

Quantum networks were proposed to transfer quantum information between distant cold atoms memories via optical links [26], and they now underpin numerous proposed applications [27]. To connect superconducting systems across such networks, a number of different microwave-to-optical transduction technologies are being investigated [28], including optomechanics [1–9,11,22,23], neutral atoms [10,12] and rare-earth-doped crystals [13–15], diamond color centers [29], and electro-optic transducers [16–21,30–33]. A critical requirement in these approaches is to optimize conversion efficiency and to minimize added noise but achieving both simultaneously is extremely challenging. Recently proposed heralded transduction from a microwave to an optical photon by heralding on a microwave Bell pair may help [25,34], but two such transduction steps would still be necessary for end-to-end state transfer, entailing high overhead. Alternatively, microwave transduction to proximal diamond color center spins has been proposed for high-speed and high-fidelity quantum network teleportation, but efficient coupling between a single spin and microwave photon has not yet been shown. By contrast, we propose a single-step, optically heralded scheme for entanglement of

two distant superconducting qubits via electro-optic parametric frequency conversion [32] based on the well-known Duan, Lukin, Cirac, and Zoller proposal [35].

Such a heralded entanglement scheme can be performed using many different M-O transduction platforms, but electro-optic transducers are particularly promising for this application. Direct electro-optic transduction provides a wide transduction bandwidth (limited only by the microwave lifetime) that enables high-rate entanglement generation even in the low M-O coupling regime. Furthermore, recent work has shown that electro-optic transducers can operate with low noise even under optical pumps exceeding $1 \mu\text{W}$ [18,20,36]. The noise in electro-optic transducers is reduced due to their physical separation of optical and microwave modes, the low thermal resistance provided by their relatively large size and nonsuspended structure, and their lack of low-frequency intermediate states.

A typical electro-optic transducer uses a $\chi^{(2)}$ nonlinear interaction between a classical optical pump mode \hat{p} , an optical mode \hat{a} , and a microwave mode \hat{b} [16,17,21,33], as illustrated in Fig. 1(a). The classical mode is red-detuned with respect to \hat{a} , leading to the Hamiltonian

$$\hat{H} = \hbar g_0 \hat{p}^\dagger \hat{a}^\dagger \hat{b} + \text{H.c.}, \quad (1)$$

where g_0 is the single-photon nonlinear interaction rate. The \hat{p} mode is classical and can be replaced by $\langle n_p \rangle$, the average number of photons in the mode. This leads to a beam-splitter-type Hamiltonian $\hat{a}^\dagger \hat{b} + \text{H.c.}$ that can be used for deterministic transduction, but its fidelity is low in practice due to the relatively low value of $g_0 \sim 1 \text{ kHz}$ compared to the optical loss rates in the system.

If the pump mode \hat{p} is instead blue-detuned, the result is two-mode squeezing. This interaction will generate pairs of optical and microwave photons via spontaneous parametric down-conversion (SPDC) [33,37–39]:

$$\hat{H} = \hbar g \hat{a} \hat{b} + \text{H.c.}, \quad (2)$$

$$g = g_0 \sqrt{\langle n_p \rangle}. \quad (3)$$

In either case, the pump power, P , is related to the number of photons in the pump mode as

$$\langle n_p \rangle = \frac{4\gamma_e}{(\gamma_e + \gamma_i)^2} \frac{P}{\hbar\omega}, \quad (4)$$

where γ_e is the extrinsic loss rate of the optical mode and γ_i is its intrinsic loss rates. Throughout the majority of this Letter, we assume the γ_e and γ_i couplings are the same for the \hat{a} and \hat{p} modes.

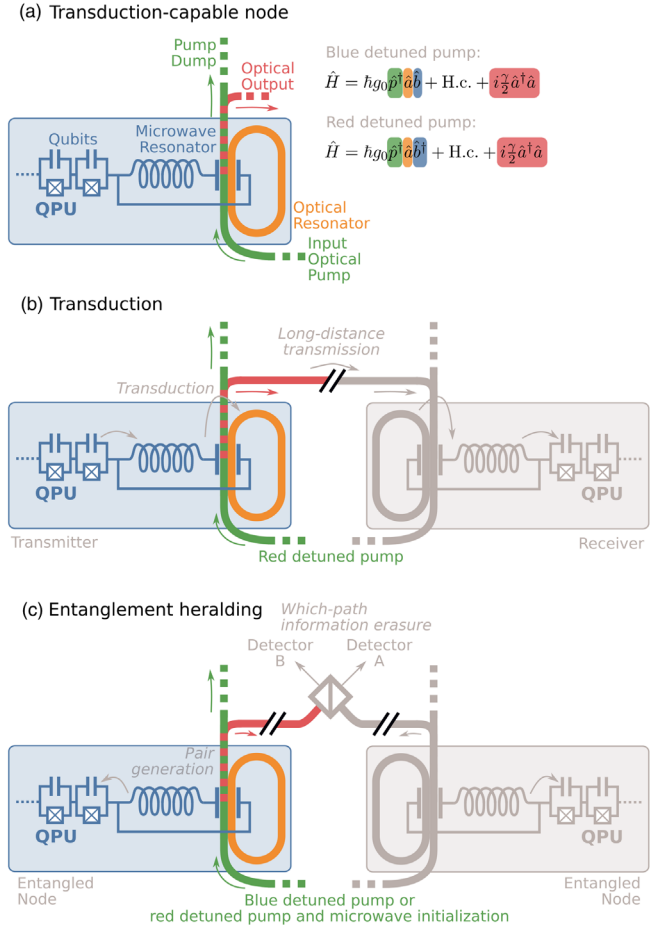


FIG. 1. (a) A typical transducer, using a $\chi^{(2)}$ process whereby a classical pump enables a beam splitter or two-mode squeezer between an optical mode and a microwave mode. (b) If the pump is red-detuned from the optical mode it enables a beam-splitter interaction that can transduce a microwave state into an optical state. This is a deterministic but low-fidelity operation. (c) If the pump is blue-detuned, it will create pairs of microwave or optical photons. By detection of the optical photons after erasing the path information, we can herald entanglement between the microwave oscillators. This is a high-fidelity, low-efficiency probabilistic operation.

If we couple the optical mode to a waveguide ending with a photodetector, this SPDC process allows us to herald the production of a single microwave photon by detecting a single optical photon. First, we will explore the performance of this procedure, and then we will examine how it enables the heralding of entanglement between two remote microwave systems. Lastly, while the blue-detuned pump is the more natural method for heralded operation, we will also explore an improved way to perform the heralding, which goes back to the use of a red-detuned pump and provides protection against certain errors.

The collapse operator that describes the detection of the optical photon is $\hat{c} = \sqrt{\gamma_e} \hat{a}$, which leads to a stochastic master equation with a non-Hermitian effective Hamiltonian given by [40–42]

$$\hat{H} = \hbar g \hat{a} \hat{b} + \text{H.c.} + i \hbar \frac{\gamma_e}{2} \hat{a}^\dagger \hat{a}. \quad (5)$$

We will initially assume that the intrinsic loss rate γ_i is negligible, so that all photons are output into the waveguide at rate γ_e (nonzero γ_i will reduce the detection efficiency but not the fidelity). The total loss rate $\gamma = \gamma_i + \gamma_e$ is typically much larger than g , which simplifies the dynamics. While this hardware constraint leads to limited fidelity even in state-of-the-art transduction devices [17], in the heralding protocol we describe it is essential to obtaining high fidelity. This is because $\gamma \gg g$ is required to ensure that the SPDC process does not populate the cavity mode with more than one photon at any time. It does, however, limit the rate of photon generation. The lifetime of the microwave oscillator is orders of magnitude longer than the characteristic times of the dynamics studied here and so we take it to be infinite in our initial analysis [43]. Once the heralded state is prepared in the microwave mode, we swap it out into one of the qubits of the superconducting quantum processing unit (QPU)—a non-linear operation at which transmon-based devices are becoming very capable.

We will denote a Fock state with n_a photons in optical mode \hat{a} and n_b in microwave mode \hat{b} as $|n_a n_b\rangle$. To obtain a $|11\rangle$ pair on which we can herald the single microwave photon, we simply pump the system. A click on the detector heralds the creation of a single photon in the microwave mode (a correct approximation as long as $g \ll \gamma_e$). Accounting for the $[\gamma_e/(\gamma_e + \gamma_i)]$ drop in efficiency when $\gamma_i \neq 0$ gives a rate of photon generation under a continuous pump of

$$r_0 = \frac{4g_0^2 \langle n_p \rangle \gamma_e}{(\gamma_e + \gamma_i)^2}, \quad (6)$$

which gives $r_0 \approx \langle n_p \rangle 10^{-2}$ Hz at typical $g_0 = 1$ kHz and $\gamma_e = \gamma_i = 100$ MHz.

The easiest way to derive this form for r_0 is to restrict oneself to the space spanned by $\{|00\rangle, |11\rangle\}$. For a state $|\psi\rangle = c_0|00\rangle + c_1|11\rangle$ we get the following ordinary differential equation:

$$\begin{pmatrix} \dot{c}_0 \\ \dot{c}_1 \end{pmatrix} = \begin{pmatrix} 0 & -ig \\ -ig^* & -\frac{\gamma_e}{2} \end{pmatrix} \begin{pmatrix} c_0 \\ c_1 \end{pmatrix}, \quad (7)$$

which leads to

$$\begin{pmatrix} c_0 \\ c_1 \end{pmatrix} = e^{-\frac{\gamma_e}{4}t} \begin{pmatrix} \frac{\gamma_e}{4g} \sinh(gt) + \cosh(gt) \\ -i \frac{g}{\gamma_e} \sinh(gt) \end{pmatrix}, \quad (8)$$

$$g' = \sqrt{\frac{\gamma_e^2}{4} - |g|^2}. \quad (9)$$

The stochastic master equation tells us that the probability of the photon remaining undetected at time t is

$$\langle \psi(t) | \psi(t) \rangle \sim e^{[2g' - (\gamma_e/2)]t} \sim e^{-[(4|g|^2)/(\gamma_e)]t}, \quad (10)$$

which indeed corresponds to a Poissonian detection process with rate r_0 .

If we use the same coherent pump to drive two separate copies of this system and erase the which-path information using a beam splitter [Fig. 1(c)], we will herald the generation of the distributed microwave Bell pair $|01\rangle \pm |10\rangle$ [35]. If the two nodes are mismatched and not calibrated, hence having different interaction rates g and couplings γ_e , the pair would look like $c_{1l}|01\rangle \pm c_{1r}|10\rangle$, where c_{1l} and c_{1r} are the coefficients for the left and right network nodes as defined in Eq. (8).

The rate at which these Bell pairs would be generated is

$$r_e = 2r_0 e^{-r_0 \Delta t} \frac{\Delta t}{\Delta t + t_r}, \quad (11)$$

where $r_0 \Delta t e^{-r_0 \Delta t}$ is the probability for a Poissonian single-click event during the interval Δt (the duration of each pump pulse). The factor of 2 comes from the fact that either of the two nodes can produce a heralded photon. Lastly, the overall rate is lowered proportionally to the duty cycle due to the finite t_r —the time necessary for the reset of the microwave cavity after each attempt (typically on the order of $1 \mu\text{s}$ [43]). Throughout the figures in this Letter, we report the maximal value of r_e after optimizing with respect to Δt . The probability of more than one event during the interval Δt is generally negligible but can lead to infidelities in this protocol at high entanglement rates.

The performance of the above method for heralding Bell pairs is depicted in Fig. 2. As already discussed, with an internal loss rate γ_i the rate of entanglement generation will be reduced by a factor of $[\gamma_e/(\gamma_e + \gamma_i)]$, while the fidelity of the obtained Bell pair is unaffected. Additionally, this heralded scheme ensures the fidelity is unchanged by insertion loss in the optical network (for example, due to fiber-transducer coupling losses) [35], although such losses may require higher in-cryostat optical pump power. Outside of the regime $g \ll \gamma$, this fidelity would be degraded for two reasons: on one hand, the SPDC process will excite states that contain more than one photon; on the other hand, there will be a small probability, $[c_1^2/(|c_0|^2 + |c_1|^2)]$, that the SPDC will simultaneously produce a photon in each of the two resonators. Both of these infidelities scale as (g/γ) . While the second source of infidelity is unavoidable, the first can be eliminated in the following way: instead of a blue-detuned pump, we can employ the traditional red-detuned pump used in transduction together with a particular state preparation procedure in the microwave hardware. When we reset the microwave cavity, we will prepare it in the state $|1\rangle$ instead of the ground state (a high-fidelity

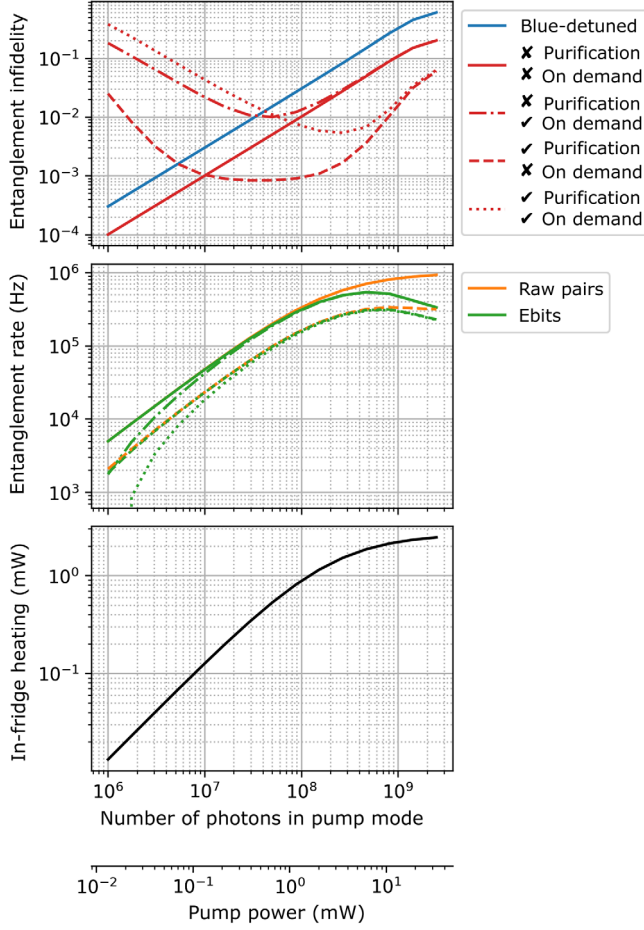


FIG. 2. In the top panel, we see the infidelity of the obtained microwave Bell pair in different regimes. The blue-detuned “squeezing” implementation has higher infidelity due to populating higher-than-one-photon states (blue line). The red-detuned “beam-splitter” implementation requires preparing the microwave resonator in the $|1\rangle$ state but does not suffer from the aforementioned excitations. We further investigate the red-detuned approach followed by purification and/or storage for on-demand use (red lines). Besides the $\sim(g/\gamma)$ infidelity in the solid lines, we see that storage at low generation rates causes an infidelity floor due to the finite microwave lifetime. The middle panel takes all red-detuned regimes from the top plot and presents their rates of entanglement generation (orange lines) and rate of equivalent ebit generation, i.e., the hashing yield [44] (green lines). The bottom panel gives the in-fridge heating due to the intrinsic loss of the optical resonator. Evaluated at $g_0 = 1\text{kHz}$, $\gamma_e = \gamma_i = 100\text{MHz}$, microwave loss $\gamma_{\text{MW}} = 1\text{kHz}$, pump wavelength $\lambda_p = 1500\text{nm}$, microwave gate fidelity 0.999, and microwave resonator reset time of $1\ \mu\text{s}$ (state-of-the-art values [17,32,43]).

operation for modern microwave hardware [43]). This leads to the same ordinary differential equation as seen in Eq. (8); however, the basis for the evolving state is now $|\psi\rangle = c_0|01\rangle + c_1|10\rangle$. Given that this Hamiltonian preserves the total photon number, it cannot excite states outside of the $\{|01\rangle, |10\rangle\}$ subspace. The same protection against multiphoton states can be achieved by keeping the

blue-detuned version of the Hamiltonian and using a strongly anharmonic microwave resonator that suppresses the two-photon excitation. As seen in Fig. 2, the elimination of unwanted multiphoton states leads to a notable increase of fidelity. Since the two resonators may still generate photons simultaneously, the residual infidelity scales as (g/γ) . The blue-detuned approach leads to a microwave entangled pair $|01\rangle \pm |10\rangle$, while in the red-detuned case with state preparation we herald a $|00\rangle \pm |11\rangle$ pair.

We estimate that typical hardware parameters of state-of-the-art devices ($\gamma_e = \gamma_i = 100\text{MHz}$ and $g_0 = 1\text{kHz}$ in [17,43]) will allow pair generation rates of 100kHz at fidelities of 0.99, while suffering 0.1 mW of in-fridge heating due to leakage from the pump. The infidelity can be lowered by an order of magnitude while incurring a decrease in the rate of just over a factor of 2 by performing a simple entanglement purification [44,45].

The entanglement rate scales as $[\gamma_e^2/(\gamma_e + \gamma_i)^4]$, which is maximal at $\gamma_e = \gamma_i$. Therefore, for a fixed pump power and in-fridge heating, the entanglement generation rate is proportional to γ_e^{-2} . The fraction of generated photons that reach the photodetector is only $[\gamma_e/(\gamma_e + \gamma_i)] = 50\%$; thus, we have to reset the microwave cavity after each attempt, a delay of $\sim 1\ \mu\text{s}$ that limits the maximal rate, as seen in the rate plot in Fig. 2.

In summary, at high entanglement rates (high pump powers), the fidelity of entanglement suffers due to undesired excitations in the nonheralded cavity, while at low rates the fidelity suffers due to the need to store the entangled pair for a long time in the microwave resonator. If we want higher rates of entanglement generation, we can counteract the fidelity drop by performing purification. Longer-term, orders of magnitude improvements in the entanglement rate or power requirements are possible through improvements in the resonator quality factor, thanks to the quadratic dependence on γ_e .

Optical pump light can produce microwave noise by direct absorption in the microwave resonator or heating the transducer node—a key challenge for all M-O transducer platforms. Several techniques can be used to reduce the effects of thermal noise in our proposed system, including light shielding [46] and immersion in a liquid helium coolant [16]. Additionally, the microwave-optical transducer can be physically connected to a 1-K stage, while radiatively overcoupling the microwave cavity mode to a thermal bath at 10 mK, as proposed in previous works [25,34,47]. This allows the transducer to use the greater cooling power of a 1-K stage while the noise is dominated by that of the colder stage. Alternatively, larger-scale custom cryostats for low-background experiments [48,49] have shown the requisite cooling power at 100 mK.

System-integration constraints—such as the desire to operate the QPU with minimal pump-light interference—could require physical separation within the cryostat between the transducer node we describe here and the

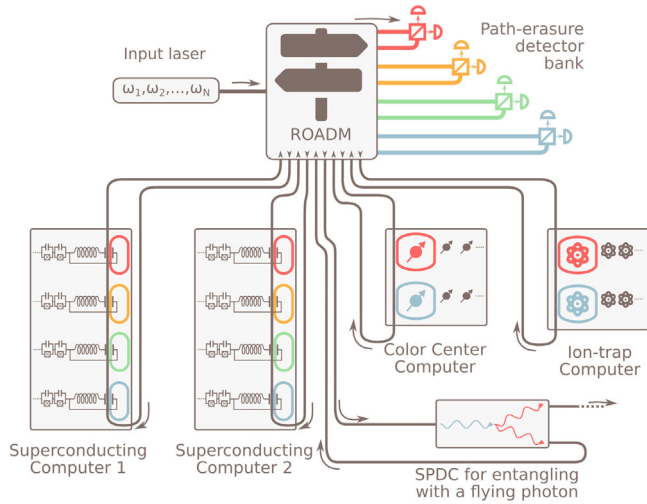


FIG. 3. Future outlook for interfridge connectivity. Replacing the single path-erasure detection with a reconfigurable optical add-drop multiplexer (ROADM) will allow us to route a frequency comb pump laser to qubits in several quantum nodes. By connecting the ROADM to a bank of path-erasure detectors for each frequency channel, this design will enable multiplexed heralded entanglement generation between multiple fridges of different quantum modalities.

main QPU. In this case, an additional pitch-and-catch transfer [50–53] of the microwave Bell state would be required. Losses during this transfer would reduce fidelity, but recent work on high-efficiency pitch-and-catch schemes suggests this loss can be made small. Dark counts due to leakage from the pump can lower the fidelity, but modern designs do not suffer from this problem (discussed in the Supplemental Material [54]).

The scheme described here extends naturally to heralding entanglement between a diverse set of quantum devices. On one hand, we can multiplex the entanglement heralding over multiple frequency channels, thus improving the entanglement generation rate. We can also use the method to entangle different quantum modalities (see Fig. 3). For example, entangling a superconducting device (where the pump, under a $\chi^{(2)}$ interaction, creates a state $|00\rangle + \varepsilon|11\rangle$) and a trapped ion device (where a conditional reflection of an attenuated pump from a $|+\rangle$ ion state creates a state $|0+\rangle + \varepsilon|1-\rangle$) in which, after path erasure, we obtain the entangled microwave-ion pair $|0+\rangle \pm |1-\rangle$. We can also herald the entanglement of the microwave cavity with a flying photon: one of the nodes is of the architecture discussed up to here, while the other node uses the pump in an SPDC photon pair generation experiment calibrated to have the same generation rate. In other words, one of the nodes can employ a microwave-optical $\chi^{(2)}$ process, while the other node employs a purely optical $\chi^{(2)}$ process, leading to heralding the entanglement of a microwave qubit and a flying optical qubit (in the single-rail basis).

As mentioned earlier in this Letter, the quantum networking community has explored transduction through heralding over O-M two-mode squeezing and entanglement before [25,30,34,59]. However, these schemes generally provide for the transduction or teleportation of a microwave state into an optical state or the same in the reverse direction. In our approach, while the hardware is virtually the same, the quantum information of interest is never truly carried by an optical mode, rather the optics is used only for the direct entanglement of two microwave modes.

In conclusion, we have proposed a method of heralded entanglement generation between remote microwave photons. Our scheme relies on SPDC using previously demonstrated electro-optic transducers tuned to the low-coupling regime such that low-efficiency generation of a microwave- and optical-photon pair is the primary transduction process. We have shown that, by heralding the optical photons from two QPUs, we can entangle the accompanying microwave photons remaining in each microwave cavity. Hence, our scheme allows for high-fidelity entanglement in the same hardware used today for low-fidelity transduction. We further demonstrate how to scale our proposed architecture to connect multiple QPUs across several quantum modalities. We believe this entanglement procedure will be valuable for the on-demand, multiplexed entanglement necessary for a quantum network.

We thank Liang Jiang, Marc Davis, Saikat Guha, Michael Fanto, Matthew LaHaye, and Lamia Ateshian for helpful discussions. The Python and Qutip open source communities provided invaluable research software. S. K. and H. R. are grateful for the funding provided by the MITRE Quantum Moonshot Program. K. J. acknowledges support from a DEVCOM Army Research Laboratory ECI grant. H. R. acknowledges support from the NSF Center for Ultracold Atoms. J. H., M. L., and M. R. acknowledge support from AFRL. J. H., D. E., and M. L. acknowledge support from NSF.

- [1] K. Stannigel, P. Rabl, A. S. Sørensen, P. Zoller, and M. D. Lukin, Optomechanical Transducers for Long-Distance Quantum Communication, *Phys. Rev. Lett.* **105**, 220501 (2010).
- [2] A. H. Safavi-Naeini and O. Painter, Proposal for an optomechanical traveling wave phonon–photon translator, *New J. Phys.* **13**, 013017 (2011).
- [3] L. Tian, Adiabatic State Conversion and Pulse Transmission in Optomechanical Systems, *Phys. Rev. Lett.* **108**, 153604 (2012).
- [4] Y.-D. Wang and A. A. Clerk, Using Interference for High Fidelity Quantum State Transfer in Optomechanics, *Phys. Rev. Lett.* **108**, 153603 (2012).
- [5] J. Bochmann, A. Vainsencher, D. D. Awschalom, and A. N. Cleland, Nanomechanical coupling between microwave and optical photons, *Nat. Phys.* **9**, 712 (2013).

- [6] T. Bağcı, A. Simonsen, S. Schmid, L. G. Villanueva, E. Zeuthen, J. Appel, J. M. Taylor, A. Sørensen, K. Usami, A. Schliesser *et al.*, Optical detection of radio waves through a nanomechanical transducer, *Nature (London)* **507**, 81 (2014).
- [7] R. W. Andrews, R. W. Peterson, T. P. Purdy, K. Cicak, R. W. Simmonds, C. A. Regal, and K. W. Lehnert, Bidirectional and efficient conversion between microwave and optical light, *Nat. Phys.* **10**, 321 (2014).
- [8] L. Tian, Optoelectromechanical transducer: Reversible conversion between microwave and optical photons, *Ann. Phys. (Amsterdam)* **527**, 1 (2015).
- [9] K. C. Balram, M. I. Davanço, J. D. Song, and K. Srinivasan, Coherent coupling between radiofrequency, optical and acoustic waves in piezo-optomechanical circuits, *Nat. Photonics* **10**, 346 (2016).
- [10] B. T. Gard, K. Jacobs, R. McDermott, and M. Saffman, Microwave-to-optical frequency conversion using a cesium atom coupled to a superconducting resonator, *Phys. Rev. A* **96**, 013833 (2017).
- [11] A. P. Higginbotham, P. Burns, M. Urmeý, R. Peterson, N. Kampel, B. Brubaker, G. Smith, K. Lehnert, and C. Regal, Harnessing electro-optic correlations in an efficient mechanical converter, *Nat. Phys.* **14**, 1038 (2018).
- [12] J. P. Covey, A. Sipahigil, and M. Saffman, Microwave-to-optical conversion via four-wave mixing in a cold ytterbium ensemble, *Phys. Rev. A* **100**, 012307 (2019).
- [13] J. G. Bartholomew, J. Rochman, T. Xie, J. M. Kindem, A. Ruskuc, I. Craiciu, M. Lei, and A. Faraon, On-chip coherent microwave-to-optical transduction mediated by ytterbium in YVO_4 , *Nat. Commun.* **11**, 3266 (2020).
- [14] S. Welinski, P. J. T. Woodburn, N. Lauk, R. L. Cone, C. Simon, P. Goldner, and C. W. Thiel, Electron Spin Coherence in Optically Excited States of Rare-Earth Ions for Microwave to Optical Quantum Transducers, *Phys. Rev. Lett.* **122**, 247401 (2019).
- [15] J. R. Everts, M. C. Berrington, R. L. Ahlefeldt, and J. J. Longdell, Microwave to optical photon conversion via fully concentrated rare-earth-ion crystals, *Phys. Rev. A* **99**, 063830 (2019).
- [16] L. Fan, C.-L. Zou, R. Cheng, X. Guo, X. Han, Z. Gong, S. Wang, and H. X. Tang, Superconducting cavity electro-optics: A platform for coherent photon conversion between superconducting and photonic circuits, *Sci. Adv.* **4**, eaar4994 (2018).
- [17] J. Holzgrafe, N. Sinclair, N. Sinclair, D. Zhu, D. Zhu, A. Shams-Ansari, M. Colangelo, Y. Hu, Y. Hu, M. Zhang, M. Zhang, K. K. Berggren, and M. Lončar, Cavity electro-optics in thin-film lithium niobate for efficient microwave-to-optical transduction, *Optica* **7**, 1714 (2020).
- [18] W. Fu, M. Xu, X. Liu, C.-L. Zou, C. Zhong, X. Han, M. Shen, Y. Xu, R. Cheng, S. Wang *et al.*, Ground-state pulsed cavity electro-optics for microwave-to-optical conversion, *Phys. Rev. A* **103**, 053504 (2021).
- [19] J. Orcutt, H. Paik, L. Bishop, C. Xiong, R. Schilling, and A. Falk, Engineering electro-optics in SiGe/Si waveguides for quantum transduction, *Quantum Sci. Technol.* **5**, 034006 (2020).
- [20] W. Hease, A. Rueda, R. Sahu, M. Wulf, G. Arnold, H. G. L. Schwefel, and J. M. Fink, Bidirectional electro-optic wavelength conversion in the quantum ground state, *PRX Quantum* **1**, 020315 (2020).
- [21] L. Fan, C. Zou, R. Cheng, X. Guo, X. Han, Z. Gong, S. Wang, and H. Tang, Cavity electro-optic circuit for microwave-to-optical frequency conversion, in *Nonlinear Optics* (Optical Society of America, 2019), pp. NF2A–2.
- [22] M. Mirhosseini, A. Sipahigil, M. Kalaei, and O. Painter, Quantum transduction of optical photons from a superconducting qubit, *Nature (London)* **588**, 599 (2020).
- [23] W. Jiang, C. J. Sarabalis, Y. D. Dahmani, R. N. Patel, F. M. Mayor, T. P. McKenna, R. Van Laer, and A. H. Safavi-Naeini, Efficient bidirectional piezo-optomechanical transduction between microwave and optical frequency, *Nat. Commun.* **11**, 1 (2020).
- [24] M. Wu, E. Zeuthen, K. C. Balram, and K. Srinivasan, Microwave-to-Optical Transduction Using a Mechanical Supermode for Coupling Piezoelectric and Optomechanical Resonators, *Phys. Rev. Applied* **13**, 014027 (2020).
- [25] C. Zhong, Z. Wang, C. Zou, M. Zhang, X. Han, W. Fu, M. Xu, S. Shankar, M. H. Devoret, H. X. Tang *et al.*, Proposal for Heralded Generation and Detection of Entangled Microwave–Optical-Photon Pairs, *Phys. Rev. Lett.* **124**, 010511 (2020).
- [26] J. I. Cirac, P. Zoller, H. J. Kimble, and H. Mabuchi, Quantum State Transfer and Entanglement Distribution among Distant Nodes in a Quantum Network, *Phys. Rev. Lett.* **78**, 3221 (1997).
- [27] S. Wehner, D. Elkouss, and R. Hanson, Quantum internet: A vision for the road ahead, *Science* **362**, eaam9288 (2018).
- [28] N. Lauk, N. Sinclair, S. Barzanjeh, J. P. Covey, M. Saffman, M. Spiropulu, and C. Simon, Perspectives on quantum transduction, *Quantum Sci. Technol.* **5**, 020501 (2020).
- [29] T. Neuman, M. Eichenfield, M. Trusheim, L. Hackett, P. Narang, and D. Englund, A phononic bus for coherent interfaces between a superconducting quantum processor, spin memory, and photonic quantum networks, *arXiv*: 2003.08383.
- [30] A. Rueda, W. Hease, S. Barzanjeh, and J. M. Fink, Electro-optic entanglement source for microwave to telecom quantum state transfer, *npj Quantum Inf.* **5**, 108 (2019).
- [31] D.-Q. Zhu and P.-B. Li, Preparation of entangled states of microwave photons in a hybrid system via the electro-optic effect, *Opt. Express* **25**, 28305 (2017).
- [32] T. P. McKenna, T. P. McKenna, J. D. Witmer, J. D. Witmer, R. N. Patel, W. Jiang, R. V. Laer, P. Arrangoiz-Arriola, E. A. Wollack, J. F. Herrmann, and A. H. Safavi-Naeini, Cryogenic microwave-to-optical conversion using a triply resonant lithium-niobate-on-sapphire transducer, *Optica* **7**, 1737 (2020).
- [33] A. Rueda, F. Sedlmeir, M. C. Collodo, U. Vogl, B. Stiller, G. Schunk, D. V. Strekalov, C. Marquardt, J. M. Fink, O. Painter *et al.*, Efficient microwave to optical photon conversion: An electro-optical realization, *Optica* **3**, 597 (2016).
- [34] C. Zhong, X. Han, H. X. Tang, and L. Jiang, Entanglement of microwave-optical modes in a strongly coupled electro-optomechanical system, *Phys. Rev. A* **101**, 032345 (2020).
- [35] L.-M. Duan, M. D. Lukin, J. I. Cirac, and P. Zoller, Long-distance quantum communication with atomic ensembles and linear optics, *Nature (London)* **414**, 413 (2001).

- [36] S. Mobassem, N. J. Lambert, A. Rueda, J. M. Fink, G. Leuchs, and H. G. L. Schwefel, Thermal noise in electro-optic devices at cryogenic temperatures, [arXiv:2008.08764](https://arxiv.org/abs/2008.08764).
- [37] C. Couteau, Spontaneous parametric down-conversion, *Contemp. Phys.* **59**, 291 (2018).
- [38] X. Guo, C.-I. Zou, C. Schuck, H. Jung, R. Cheng, and H. X. Tang, Parametric down-conversion photon-pair source on a nanophotonic chip, *Light* **6**, e16249 (2017).
- [39] A. Rueda, Frequency multiplexed optical entangled source based on the Pockels effect, *Phys. Rev. A* **103**, 023708 (2021).
- [40] R. Dum, P. Zoller, and H. Ritsch, Monte Carlo simulation of the atomic master equation for spontaneous emission, *Phys. Rev. A* **45**, 4879 (1992).
- [41] K. Mølmer, Y. Castin, and J. Dalibard, Monte Carlo wavefunction method in quantum optics, *J. Opt. Soc. Am. B* **10**, 524 (1993).
- [42] K. Jacobs, *Quantum Measurement Theory and its Applications* (Cambridge University Press, Cambridge, 2014).
- [43] M. Kjaergaard, M. E. Schwartz, J. Braumüller, P. Krantz, J. I.-J. Wang, S. Gustavsson, and W. D. Oliver, Superconducting qubits: Current state of play, *Annu. Rev. Condens. Matter Phys.* **11**, 369 (2020).
- [44] C. H. Bennett, D. P. DiVincenzo, J. A. Smolin, and W. K. Wootters, Mixed-state entanglement and quantum error correction, *Phys. Rev. A* **54**, 3824 (1996).
- [45] S. Krastanov, V. V. Albert, and L. Jiang, Optimized entanglement purification, *Quantum* **3**, 123 (2019).
- [46] J. M. Kreikebaum, A. Dove, W. Livingston, E. Kim, and I. Siddiqi, Optimization of infrared and magnetic shielding of superconducting TiN and Al coplanar microwave resonators, *Supercond. Sci. Technol.* **29**, 104002 (2016).
- [47] M. Xu, X. Han, C.-L. Zou, W. Fu, Y. Xu, C. Zhong, L. Jiang, and H. X. Tang, Radiative Cooling of a Superconducting Resonator, *Phys. Rev. Lett.* **124**, 033602 (2020).
- [48] V. Singh, C. Alduino, F. Alessandria, A. Bersani, M. Biassoni, C. Bucci, A. Caminata, L. Canonica, L. Cappelli, R. Cereseto *et al.*, The CUORE cryostat: Commissioning and performance, *J. Phys. Conf. Ser.* **718**, 062054 (2016).
- [49] C. Davis, Search for neutrinoless double-beta decay with Majoron emission in CUORE, Ph.D. thesis, Yale University, 2020.
- [50] P. Campagne-Ibarcq, E. Zalys-Geller, A. Narla, S. Shankar, P. Reinhold, L. Burkhardt, C. Axline, W. Pfaff, L. Frunzio, R. J. Schoelkopf, and M. H. Devoret, Deterministic Remote Entanglement of Superconducting Circuits through Microwave Two-Photon Transitions, *Phys. Rev. Lett.* **120**, 200501 (2018).
- [51] J. Wenner, Y. Yin, Y. Chen, R. Barends, B. Chiaro, E. Jeffrey, J. Kelly, A. Megrant, J. Y. Mutus, C. Neill *et al.*, Catching Time-Reversed Microwave Coherent State Photons with 99.4% Absorption Efficiency, *Phys. Rev. Lett.* **112**, 210501 (2014).
- [52] C. J. Axline, L. D. Burkhardt, W. Pfaff, M. Zhang, K. Chou, P. Campagne-Ibarcq, P. Reinhold, L. Frunzio, S. Girvin, L. Jiang *et al.*, On-demand quantum state transfer and entanglement between remote microwave cavity memories, *Nat. Phys.* **14**, 705 (2018).
- [53] P. Kurpiers, P. Magnard, T. Walter, B. Royer, M. Pechal, J. Heinsoo, Y. Salathé, A. Akin, S. Storz, J.-C. Besse *et al.*, Deterministic quantum state transfer and remote entanglement using microwave photons, *Nature (London)* **558**, 264 (2018).
- [54] See Supplemental Material at <http://link.aps.org/supplemental/10.1103/PhysRevLett.127.040503>, which includes Refs. [45,55–58] for possible pump filter designs, entanglement purification protocols, and effects due to changes in the local gate fidelity.
- [55] F. Marsili, V. B. Verma, J. A. Stern, S. Harrington, A. E. Lita, T. Gerrits, I. Vayshenker, B. Baek, M. D. Shaw, R. P. Mirin *et al.*, Detecting single infrared photons with 93% system efficiency, *Nat. Photonics* **7**, 210 (2013).
- [56] E. A. Dauler, M. E. Grein, A. J. Kerman, F. Marsili, S. Miki, S. W. Nam, M. D. Shaw, H. Terai, V. B. Verma, and T. Yamashita, Review of superconducting nanowire single-photon detector system design options and demonstrated performance, *Opt. Eng.* **53**, 081907 (2014).
- [57] C. Wang, M. Zhang, M. Yu, R. Zhu, H. Hu, and M. Loncar, Monolithic lithium niobate photonic circuits for Kerr frequency comb generation and modulation, *Nat. Commun.* **10**, 1 (2019).
- [58] M. Piekarek, D. Bonneau, S. Miki, T. Yamashita, M. Fujiwara, M. Sasaki, H. Terai, M. G. Tanner, C. M. Natarajan, R. H. Hadfield *et al.*, High-extinction ratio integrated photonic filters for silicon quantum photonics, *Opt. Lett.* **42**, 815 (2017).
- [59] S. Barzanjeh, M. Abdi, G. J. Milburn, P. Tombesi, and D. Vitali, Reversible Optical-to-Microwave Quantum Interface, *Phys. Rev. Lett.* **109**, 130503 (2012).